

---

# AR-DIFFUSION: Auto-Regressive Diffusion Model for Text Generation

---

Tong Wu<sup>1\*†</sup>, Zhihao Fan<sup>2\*†</sup>, Xiao Liu<sup>3</sup>, Yeyun Gong<sup>3‡</sup>, Yelong Shen<sup>4</sup>, Jian Jiao<sup>4</sup>, Hai-Tao Zheng<sup>1‡</sup>, Juntao Li<sup>5</sup>, Zhongyu Wei<sup>2</sup>, Jian Guo<sup>6</sup>, Nan Duan<sup>3‡</sup>, Weizhu Chen<sup>4</sup>

<sup>1</sup>Shezhen International Graduate School, Tsinghua University, <sup>2</sup>Fudan University,

<sup>3</sup>Microsoft Research Asia, <sup>4</sup>Microsoft, <sup>5</sup>Soochow University, <sup>6</sup>IDEA Research,

{yegong, yeshe, nanduan, wzchen}@microsoft.com,

zheng.haitao@sz.tsinghua.edu.cn

## Abstract

Diffusion models have gained significant attention in the realm of image generation due to their exceptional performance. Their success has been recently expanded to text generation via generating all tokens within a sequence concurrently. However, natural language exhibits a far more pronounced sequential dependency in comparison to images, and the majority of existing language models are trained utilizing a left-to-right auto-regressive approach. To account for the inherent sequential characteristic of natural language, we introduce Auto-Regressive Diffusion (AR-DIFFUSION). AR-DIFFUSION ensures that the generation of tokens on the right depends on the generated ones on the left, a mechanism achieved through employing a dynamic number of denoising steps that vary based on token position. This results in tokens on the left undergoing fewer denoising steps than those on the right, thereby enabling them to generate earlier and subsequently influence the generation of tokens on the right. In a series of experiments on various text generation tasks including text summarization, machine translation, and common sense generation, AR-DIFFUSION clearly demonstrated the superiority over existing diffusion language models and that it can be  $100\times \sim 600\times$  faster when achieving comparable results. Our code will be publicly released.

## 1 Introduction

Text generation is a fundamental task within the field of natural language processing (NLP). Pre-trained language models like GPT-4 [OpenAI, 2023], LLaMA [Touvron et al., 2023], and Alpaca [Taori et al., 2023] have garnered significant attention with their ability to generate fluent and human-like textual content. These models utilize the auto-regressive (AR) Transformer decoders [Vaswani et al., 2017] to emit generated tokens one-by-one in sequential order from left to right. By leveraging the power of position dependency, AR models are able to enhance the naturalness, coherence, and adherence to human language conventions in the generated text [Brown et al., 2020].

Recent studies have shown the remarkable performance of diffusion model in image generation [Ho et al., 2020], motivating researchers to extend diffusion to text generation [Li et al., 2022a, Gong et al., 2022, Dieleman et al., 2022, Yuan et al., 2022, Ye et al., 2023]. By introducing timestep, these methods progressively regulate the interpolation between the original tokens and Gaussian noise, then iteratively denoise for text generation. At each timestep, the diffusion-based text generator predicts all tokens simultaneously following Non-Auto-Regression (NAR), leading to faster decoding

---

\*Work done during an internship at Microsoft Research Asia.

†These authors contributed equally to this work.

‡Corresponding author.

speed compared to AR [Lewis et al., 2020, Qi et al., 2020, 2021, Li et al., 2022b]. However, it also inherits the drawback of NAR, namely the sacrifice of inter-token position dependency [Li et al., 2022c] and the drop of generation performance [Bao et al., 2021].

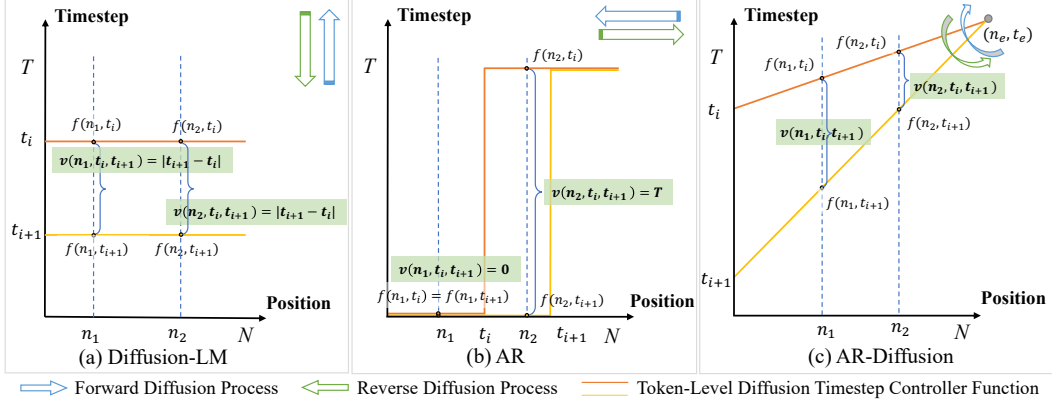


Figure 1: Model behaviors illustrated on a two-dimensional coordinate system, where the horizontal axis stands for the position and the vertical axis represents the diffusion timestep. In the inference stage, different models will behave differently. (a) For the typical Diffusion-LM [Li et al., 2022a], each token share the identical movement speed  $v(n_1, t_i, t_{i+1}) = v(n_2, t_i, t_{i+1}) = |t_{i+1} - t_i|$ . (b) For AR from the perspective of diffusion models, the tokens have two states based on the degree of interpolation between the original tokens and Gaussian noise: to be decoded (at timestep  $t = T$ ) and already decoded (at timestep  $t = 0$ ). Specifically, we have  $v(n_1, t_i, t_{i+1}) = 0$  and  $v(n_2, t_i, t_{i+1}) = T$ . (c) In AR-DIFFUSION,  $(n_e, t_e)$  is the coordinate of anchor point. The movement speeds of different tokens are different, such as  $v(n_1, t_i, t_{i+1}) > v(n_2, t_i, t_{i+1})$  when  $n_1 < n_2$ .

To conduct a comprehensive analysis, we introduce a two-dimensional coordinate system to track the diffusion timestep of tokens  $f(\cdot)$  positioned at various locations. As illustrated in Figure 1, the system assigns the token position  $n \in [1, N]$  to the horizontal axis and the diffusion timestep  $t \in [0, T]$  to the vertical axis. Diffusion-LM [Li et al., 2022a], which is followed by existing diffusion-based text generation models, is shown in Figure 1(a). It assigns a uniform timestep  $t$  to all tokens. In contrast, tokens in the AR model depicted in Figure 1(b) exhibit distinct timesteps within a generation step ( $t_i$ ). For instance, the already decoded token at position  $n_1$  has a timestep of 0, while the to-be-decoded token at position  $n_2$  has a timestep of  $T$ . This approach effectively captures the sequential order. Motivated by this observation, we introduce AR-DIFFUSION, an auto-regressive diffusion method, for the disparity in token positions and the principle of sequential token identification.

In AR-DIFFUSION, we propose a **multi-level diffusion strategy** that includes both sentence-level and token-level diffusion. We randomly choose a sentence-level timestep  $t$ , and assign **dynamic movement speeds**  $v(\cdot)$  by determining position-sensitive token-level timestep  $f(n, t)$  for each token. This enables tokens at the beginning of a sentence to undergo faster movement from random Gaussian noise to token embedding, while those at the end of the sentence experience slower movement to better utilize information from previously denoised tokens. During inference, to reduce the significant number of inference steps (e.g., 2,000) required in Diffusion-LM [Li et al., 2022a], SeqDiffSeq [Yuan et al., 2022] and GENIE [Lin et al., 2023], we introduce a skipping mechanism that collaborates with the multi-level diffusion strategy to accelerate the process.

Experimental results across various text generation tasks, such as text summarization, machine translation, and common sense generation, have consistently demonstrated that AR-DIFFUSION surpasses existing text diffusion models, including AR methods in terms of both quality and diversity. Moreover, our verification reveals that AR-DIFFUSION requires fewer resources during decoding while maintaining superior performance. It achieves  $100\times$  faster than SeqDiffSeq [Yuan et al., 2022] and  $600\times$  faster than GENIE [Lin et al., 2023] while delivering comparable results. Furthermore, it demonstrates promising results even in a challenging scenario where decoding is limited to only two timesteps.

## 2 Preliminary

### 2.1 Conditional Generative Language Models

In the field of natural language generation, conditional generative models are commonly implemented using either auto-regressive (AR) or non-auto-regressive (NAR) methods. In AR [Vaswani et al., 2017], tokens on the right are predicted based on visible left tokens. The likelihood is given by  $p_{\text{AR}}(\mathbf{y}|\mathbf{x}) = \prod_{i=1}^N p(\mathbf{y}_i|\mathbf{y}_{1:i-1}; \mathbf{x})$ , where  $y_i$  denotes the  $i$ -th token of  $\mathbf{y}$ . On the other hand, NAR [Gu et al., 2017] assumes conditional independence among tokens and generates them uniformly without distinction during decoding, resulting in the likelihood  $p_{\text{NAR}}(\mathbf{y}|\mathbf{x}) = \prod_{i=1}^N p(\mathbf{y}_i|\mathbf{x})$ . This parallel generation approach is of lower quality compared to AR, although it offers a substantial speed advantage.

### 2.2 Diffusion Models for Text Generation

Recently, Li et al. [2022a] proposes a natural language generation model based on the diffusion process, which is typically divided into forward noising process and reverse denoising process.

Specifically, the forward process is a fixed linear Gaussian model, which gradually perturbs the random variable  $\mathbf{z}_0$  until it becomes the standard Gaussian distribution. This can be formalized as:

$$q(\mathbf{z}_t | \mathbf{z}_0; \mathbf{x}) = \mathcal{N}(\mathbf{z}_t; \sqrt{\bar{\alpha}_t}\mathbf{z}_0, (1 - \bar{\alpha}_t)\mathbf{I}) \quad (1)$$

where,  $\bar{\alpha}_t = \prod_{i=1}^t \alpha_i$ , where  $\alpha_i$  is a coefficient that monotonically decreases with timestep  $t$ , and  $\mathbf{z}_t$  is the state at timestep  $t$ .

The reverse process is to initiate from standard Gaussian noise and progressively utilize the denoising transition  $p_{\theta}(\mathbf{z}_{t-1}|\mathbf{z}_t; \mathbf{x})$  for generation.

$$p_{\theta}(\mathbf{z}_{t-1} | \mathbf{z}_t; \mathbf{x}) = \mathcal{N}(\mathbf{z}_{t-1}; \mu_{\theta}(\mathbf{z}_t, t; \mathbf{x}), \Sigma_{\theta}(\mathbf{z}_t, t; \mathbf{x})) \quad (2)$$

where the mean  $\mu_{\theta}$  and variance  $\Sigma_{\theta}$  are learned from the model. In particular, we follow Li et al. [2022a]’s approach of using predefined variance without trainable parameters.

To extend the continuous diffusion process to discrete text generation, Li et al. [2022a] introduces an additional Markov transition from the discrete tokens  $\mathbf{y}$  to the latent variable  $\mathbf{z}_0$ . In practice, we add an embedding step  $q_{\phi}(\mathbf{z}_0|\mathbf{y}) = \mathcal{N}(\mathbf{z}_0; \text{Emb}(\mathbf{y}), (1 - \alpha_0)\mathbf{I})$  in the forward process, and use a trainable rounding step which is parametrized by  $p_{\theta}(\mathbf{y}|\mathbf{z}_0; \mathbf{x}) = \prod_{i=1}^N p_{\theta}(y_i|\mathbf{z}_0^i; \mathbf{x})$  in the reverse process. In each timestep, we utilize an encoder-decoder model  $\mathbf{g}_{\theta}(\mathbf{z}_t, t; \mathbf{x})$  to approximate  $\mathbf{z}_0$  [Lin et al., 2023] in a NAR manner and then estimate  $\mu_{\theta}(\mathbf{z}_t, t; \mathbf{x})$ .

In consequence, combined with maximizing the evidence lower bound (ELBO) of  $\log p_{\theta}(\mathbf{y}|\mathbf{x})$ , our training objective of the conditional diffusion language model is:

$$\mathcal{L} = \mathbb{E}_{q_{\phi}(\mathbf{z}_{0:T}|\mathbf{y})} \left[ -\log p_{\theta}(\mathbf{y} | \mathbf{z}_0; \mathbf{x}) + \sum_{t=1}^T \|\mathbf{z}_0 - \mathbf{g}_{\theta}(\mathbf{z}_t, t; \mathbf{x})\|^2 \right] \quad (3)$$

## 3 Methodology

### 3.1 Multi-level Diffusion

The typical diffusion process assumes that each token in the text-sequence has the same diffusion time-step. To leverage the sequential nature of language, we propose to allow tokens to be at different diffusion time-steps during the forward/backward pass. For example, it would make the tokens at the beginning of sentence decode earlier than the tokens at the end. To achieve that, AR-DIFFUSION adopts a two-level diffusion, which comprise two levels: sentence-level diffusion and token-level diffusion. Firstly, at the sentence-level diffusion, we follow the Diffusion-LM [Li et al., 2022a] to randomly select a timestep  $t$ . Secondly, at the token-level diffusion, we incorporate positional information  $n \in [1, N]$  based on the sentence-level timestep to regulate the diffusion timestep for the current token. The procedure is illustrated as:

$$\mathbf{z}_t = (\mathbf{z}_{f(1,t)}^1, \mathbf{z}_{f(2,t)}^2, \dots, \mathbf{z}_{f(N,t)}^N), \quad (4)$$

---

**Algorithm 1** Training Process of AR-DIFFUSION.

---

**Input:** Dataset  $\{(\mathbf{x}, \mathbf{y})\}$ , maximum timestep number  $T$  and maximum target length  $N$ .

**Output:** Optimized model parameters  $\theta$ .

1: Define an anchor point  $(n_e, t_e)$ .

2: **repeat**

3: Sample  $(\mathbf{x}, \mathbf{y})$  from the dataset and embed  $\mathbf{y}$  into  $\mathbf{z}_0$ .

4: Sample a sentence-level timestep  $t$  from the interval  $[0, N + T]$ , then the start point is determined by the following equation:

$$(n_s, t_s) = (\text{clip}(N - t, 0, N), \text{clip}(t - N, 0, T)) \quad (6)$$

5: Use the point-slope linear function to determine the token-level timestep  $f(n, t)$  in position  $n$ :

$$f(n, t) = \text{clip}\left(\frac{t_e - t_s}{n_e - n_s}(n - n_s) + t_s, 0, T\right) \quad (7)$$

6: Sample  $\mathbf{z}_{f(n,t)}^n$  for each  $n$  in different positions with Gaussian reparameterization.

7: According to equation (3) and equation (9), employ gradient descent to optimize the objective:

$$\min_{\theta} \left[ -\log p_{\theta}(\mathbf{y} | \mathbf{z}_0; \mathbf{x}) + \sum_{n=1}^N \|\mathbf{g}_{\theta}(\mathbf{z}_{f(n,t)}^n, f(n, t); \mathbf{x}) - \mathbf{z}_0\|^2 \right] \quad (8)$$

8: **until** converged

---

where  $N$  is the given target sentence length,  $\mathbf{z}_t$  is the sentence representation at timestep<sup>4</sup>  $t$ ,  $\mathbf{z}_t^i$  is the latent representation for the  $i$ -th token at timestep  $t$ , and  $f(n, t)$  is a token-level timestep controller function that denotes the token-level diffusion timestep determined by token position  $n$  and sentence-level timestep  $t$ .

We visualize the token-level timestep  $(n, f(n, t))$  onto a two-dimensional coordinate system, which takes the token **position** as the horizontal axis and the sentence-level **timestep** as the vertical axis. Furthermore, To provide a more profound description of the characteristics of movement, we define the speed of movement as the following equation.

$$v(n, t_i, t_{i+1}) = f(n, t_{i+1}) - f(n, t_i) \quad (5)$$

where  $t_i$  and  $t_{i+1}$  are the start and end sentence-level diffusion timesteps. We illustrate the examples of Diffusion-LM [Li et al., 2022a] and AR in Figure 1 (a) and (b).

### 3.2 Token-Level Diffusion with Dynamic Movement Speed

To take advantage of AR in diffusion, we propose a key principle for designing the token-level diffusion timestep function  $f(n, t)$ . Specifically, elements at the left of a sentence undergo faster movement from random Gaussian noise to token embedding, while those at the right of the sentence undergo slower movement, thereby utilizing information from previously generated words.

We devise a token-level diffusion strategy based on the linear function, which is shown in Figure 1(c). In particular, the procedure is illustrated in Algorithm 1, where  $\text{clip}(x, \min, \max)$  function is to clamp all elements in  $x$  into the range  $[\min, \max]$ . Specifically, in forward process of diffusion, the start point goes to the left from  $(N, 0)$  to  $(0, 0)$  along the horizontal axis and then moves up to  $(0, T)$  along the vertical axis. Therefore, the entire range of sentence-level timestep is extended to  $t \in [0, N + T]$ .

While in the reverse diffusion process<sup>5</sup>, the multi-level diffusion follows the formular:

$$\mathbf{g}_{\theta}(\mathbf{z}_t, t; \mathbf{x}) = \mathbf{g}_{\theta}\left(\left(\mathbf{z}_{f(1,t)}^1, f(1, t)\right), \left(\mathbf{z}_{f(2,t)}^2, f(2, t)\right), \dots, \left(\mathbf{z}_{f(N,t)}^N, f(N, t)\right); \mathbf{x}\right) \quad (9)$$

where  $\mathbf{g}_{\theta}(\mathbf{z}_{f(n,t)}^n, f(n, t); \mathbf{x})$  is the  $n$ -th element.

---

<sup>4</sup>Please note that if we talk about a “timestep” without explicitly indicating that it is for token-level, it should be for sentence-level.

<sup>5</sup>In particular, the anchor point is set as  $(2 \times N, T)$  in our implementation.

---

**Algorithm 2** Inference Process of AR-DIFFUSION with the Skipping Mechanism.

---

**Input:** Source condition  $\mathbf{x}$ , number of decoding steps  $M$  and model parameters  $\theta$ .

**Output:** Predicted target embedding  $\hat{\mathbf{y}}$ .

- 1: Define an anchor point  $(n_e, t_e)$ .
- 2: Uniformly select a decreasing sequence of timesteps  $\{t_i\}_{i=0}^M$  ranging from  $T + N$  to 0.
- 3: Sample  $\mathbf{z}_{t_0} \sim \mathcal{N}(\mathbf{0}, \mathbf{I})$ .
- 4: **for**  $i = 0$  to  $M - 1$  **do**
- 5:   Calculate the start point  $(n_s, t_s)$  using equation (6).
- 6:   Based on the current sentence-level inference steps  $t_i$  and the next one  $t_{i+1}$ , assign token-level timesteps  $f(n, t_i)$  and  $f(n, t_{i+1})$  to token in position  $n$  using equation (7).
- 7:   Reverse sample  $\mathbf{z}_{t_{i+1}} = (\mathbf{z}_{f(1, t_{i+1})}^1, \mathbf{z}_{f(2, t_{i+1})}^2, \dots, \mathbf{z}_{f(N, t_{i+1})}^N)$  from  $p_\theta(\mathbf{z}_{t_{i+1}} \mid \mathbf{z}_{t_i}; \mathbf{x})$  with the following formulas:

$$p_\theta(\mathbf{z}_{t_{i+1}} \mid \mathbf{z}_{t_i}; \mathbf{x}) = \prod_{n=1}^N p_\theta(\mathbf{z}_{f(n, t_{i+1})}^n \mid \mathbf{z}_{f(n, t_i)}^n; \mathbf{x}) \quad (10)$$

$$p_\theta(\mathbf{z}_{f(n, t_{i+1})}^n \mid \mathbf{z}_{f(n, t_i)}^n; \mathbf{x}) \sim \mathcal{N}(\mathbf{z}_{f(n, t_{i+1})}^n; \lambda \mathbf{z}_{f(n, t_i)}^n + \mu \mathbf{g}_\theta(\mathbf{z}_{f(n, t_i)}^n, f(n, t_i); \mathbf{x}), \sigma \mathbf{I}) \quad (11)$$

8: **end for**

9: Map  $\mathbf{z}_{t_M}$  to the nearest embedding  $\hat{\mathbf{y}}$ .

---

### 3.3 Inference with Skipping

Typically, we need to go through all the sentence-level timesteps from  $T + N$  to 0. With the skipping mechanism, we only need to go through a subset of timesteps, decreasing the decoding time.

In practice, we propose an algorithm for the inference is illustrated in Algorithm 2.

$$\lambda = \frac{\sqrt{\frac{\bar{\alpha}_{f(n, t_i)}}{\bar{\alpha}_{f(n, t_{i+1})}}(1 - \bar{\alpha}_{f(n, t_{i+1})})}}{1 - \bar{\alpha}_{f(n, t_i)}}, \mu = \frac{\sqrt{\bar{\alpha}_{f(n, t_{i+1})}(1 - \frac{\bar{\alpha}_{f(n, t_i)}}{\bar{\alpha}_{f(n, t_{i+1})})}}{1 - \bar{\alpha}_{f(n, t_i)}}, \sigma = \frac{(1 - \alpha_{f(n, t_i)})(1 - \bar{\alpha}_{f(n, t_{i+1})})}{1 - \bar{\alpha}_{f(n, t_i)}} \quad (12)$$

In equation (10), the conditional distribution of  $\mathbf{z}_{t_{i+1}}$  is approximated by  $p_\theta(\mathbf{z}_{t_{i+1}} \mid \mathbf{z}_{t_i}; \mathbf{x})$ , and then decomposed by positions because the forward process of elements in different positions is independent of each other. For equation (11) ~ equation (12), the detailed derivation is available in Appendix A.

## 4 Experiments

### 4.1 Tasks and Datasets

**Text Summarization** This task involves taking a long document as input and generating a concise sentence as output. This requires models with the ability to identify important content and rewrite it in a condensed form. In our experiments we use the publicly available XSUM [Narayan et al., 2018] and CNN/DAILYMAIL Hermann et al. [2015] on GLGE<sup>6</sup>, which is also named as GLGE-Easy.

**Machine Translation** Translation is a widely used sequence-to-sequence task. The input is a sequence of words in the source language, and the output is a sequence of corresponding words in the target language. We choose the IWSLT 2014 dataset and the data processing method is to follow the scripts provided by fairseq<sup>7</sup>.

**Common Sense Generation** In this task, the model is provided with a concept set consisting of objects and actions as input. The objective is to generate a sentence that incorporates these concepts and describes a realistic scenario. We use COMMONGEN<sup>8</sup> dataset for evaluation.

---

<sup>6</sup><https://microsoft.github.io/glge/>

<sup>7</sup><https://github.com/facebookresearch/fairseq/tree/main/examples/translation>

<sup>8</sup><https://inklab.usc.edu/CommonGen/>

## 4.2 Experimental Details

**Model Setup** Our model configuration is implemented based on Transformer-base [Vaswani et al., 2017]. In particular, For XSUM and CNN/DAILYMAIL, we set the diffusion embedding dimension to 128. For IWSLT14, we use 64-dimensional diffusion embedding, 4 attention heads and 1024-dimensional feed-forward layers. For COMMONGEN, we adopt 64-dimensional diffusion embedding, 8 attention heads and 512-dimensional feed-forward layers.

**Training and Inference** In the training phase, we employ a square-root noise schedule and 2,000 diffusion steps [Li et al., 2022a]. Specially, we use the tokenizer and vocabulary constructed by Byte Pair Encoding (BPE) <sup>9</sup> [Kudo and Richardson, 2018] for translation tasks. For other tasks, we adopt the tokenizer and vocabulary of bert-base-uncased.

**Baselines** We set four groups of baselines:

- NAR: NAT [Gu et al., 2017], iNAT [Lee et al., 2018], CMLM [Ghazvininejad et al., 2019], LevT [Gu et al., 2019] and CNAT [Bao et al., 2021];
- Semi-NAR: InsT [Stern et al., 2019], iNAT [Lee et al., 2018], CMLM [Ghazvininejad et al., 2019] and LevT [Gu et al., 2019];
- AR: bRNN [Gu et al., 2016], LSTM [Greff et al., 2017] and Transformer [Vaswani et al., 2017];
- Diffusion: DiffusionLM [Li et al., 2022a], CDCD [Dieleman et al., 2022], SeqDiffuSeq [Yuan et al., 2022], DINOISER [Ye et al., 2023] and GENIE [Lin et al., 2023].

**Metrics** We follow Qi et al. [2020] <sup>10</sup> to evaluate the **ROUGE-1/2/L** of the summarization task. For the evaluation of translation tasks, we adopt the setting of SeqDiffuSeq [Yuan et al., 2022] to report BLEU score. In addition, we also calculate the SacreBLEU score according to the setting of DINOISER [Ye et al., 2023] for comparison. For COMMONGEN, we employ ROUGE-2/L, BLEU-3/4, METEOR and SPICE under the evaluation methods of Lin et al. [2020] <sup>11</sup>.

**Training Parameters** Our training parameters on different datasets are shown in Table 1. Our linear schedule warm up steps is  $4,000 \times N_{gc}$ , where  $N_{gc}$  denotes gradient accumulation number. In addition, we use the AdamW (weight decay = 0.0) optimizer and dropout is 0.2. All experiments are implemented on 8 Tesla V100-32G. It takes about 20 hours to train XSUM and CNN/DAILYMAIL, about 5 hours to train IWSLT14, and about 2 hours to train COMMENGEN.

Table 1: Training Parameter Settings. Batch Size = mini batch size  $\times N_{gc} \times$  GPU number, Optimized Steps = total steps /  $N_{gc}$ .

Dataset	Lr & Schedule	Batch Size	Optimized Steps	Target Length
XSUM	8e-4 & Cosine	128 $\times$ 3 $\times$ 8	80,000 / 3	50
CNN/DAILYMAIL	8e-4 & Cosine	80 $\times$ 5 $\times$ 8	100,000 / 5	180
IWSLT14 DE $\rightarrow$ EN	2e-3 & Cosine	192 $\times$ 2 $\times$ 8	160,000 / 2	90
IWSLT14 EN $\rightarrow$ DE	1.8e-3 & Cosine	768 $\times$ 1 $\times$ 8	60,000	90
COMMONGEN	3e-4 & Constant	384 $\times$ 1 $\times$ 8	40,000	54

## 4.3 Main Results

The results on different datasets are shown in Table 2, Table 3, Table 4 and Table 6. The best result is **bolded** and the second-best result is underlined. “*n*” indicates the number of candidate samples used for MBR decoding. It can be seen from the results in each table that AR-DIFFUSION achieves State-Of-The-Art results.

<sup>9</sup>We train bpe on the training set, and follow the vocabulary size of fairseq, IWSLT14 is set to 10,000.

<sup>10</sup>[https://github.com/microsoft/ProphetNet/tree/master/GLGE\\_baselines](https://github.com/microsoft/ProphetNet/tree/master/GLGE_baselines)

<sup>11</sup>[https://github.com/INK-USC/CommonGen/tree/master/evaluation/Traditional/eval\\_metrics](https://github.com/INK-USC/CommonGen/tree/master/evaluation/Traditional/eval_metrics)

During the inference process, our inference steps is **20** and apply Minimum Bayes Risk (MBR) [Kumar and Byrne, 2004] decoding to pick out the best sample following [Li et al., 2022a]. Since GENIE picks generated samples by calculating the maximum score with ground truth, which is quite different from our method of picking between generated samples (i.e., ground truth is completely invisible) via MBR. Therefore, we re-implemented GENIE following our model configuration and apply 20 steps to inference.

Table 2: Results on XSUM test set. The results of NAR and Semi-NAR are from Qi et al. [2021], and the results of AR are from GLGE [Liu et al., 2021].

Methods	Pattern	ROUGE-1	ROUGE-2	ROUGE-L
NAT [Gu et al., 2017]	NAR	24.0	3.9	20.3
iNAT [Lee et al., 2018]		24.0	4.0	20.4
CMLM [Ghazvininejad et al., 2019]		23.8	3.6	20.2
LevT [Gu et al., 2019]		24.8	4.2	20.9
InsT [Stern et al., 2019]	Semi-NAR	17.7	5.2	16.1
iNAT [Lee et al., 2018]		27.0	6.9	22.4
CMLM [Ghazvininejad et al., 2019]		29.1	7.7	23.0
LevT [Gu et al., 2019]		25.3	7.4	21.5
LSTM [Greff et al., 2017]	AR <sup>12</sup>	25.1	6.9	19.9
Transformer [Vaswani et al., 2017]		30.5	<u>10.4</u>	24.2
GENIE ( $n = 50$ ) [Lin et al., 2023]	Diffusion	29.3	8.3	21.9
AR-DIFFUSION ( $n = 50$ )		<u>31.7</u>	10.1	<u>24.7</u>
AR-DIFFUSION ( $n = 500$ )		<b>32.2</b>	<b>10.6</b>	<b>25.2</b>

Table 3: Results on CNN/DAILYMAIL test set. The results of AR are from GLGE Liu et al. [2021].

Methods	Pattern	ROUGE-1	ROUGE-2	ROUGE-L
LSTM [Greff et al., 2017]	AR	37.3	15.7	34.4
Transformer [Vaswani et al., 2017]		39.5	<u>16.7</u>	36.7
GENIE [Lin et al., 2023] ( $n = 50$ )	Diffusion	34.4	12.8	32.1
AR-DIFFUSION ( $n = 50$ )		<u>39.6</u>	16.3	<u>37.1</u>
AR-DIFFUSION ( $n = 500$ )		<b>40.2</b>	<b>17.1</b>	<b>37.7</b>

**Text Summarization** The results presented in Table 2 and Table 3 clearly demonstrate that AR-DIFFUSION outperforms the existing NAR and Semi-NAR approaches across all metrics. Moreover, AR-DIFFUSION consistently achieves significant improvements over GENIE in terms of all indicators. Furthermore, in comparison to Transformer, AR-DIFFUSION outperforms it both ROUGE-1 and ROUGE-L, while achieving comparable performance in terms of ROUGE-2. Notably, when  $n$  is 500, AR-DIFFUSION demonstrates superiority over Transformer involving all measures.

Table 4: Results on IWSLT14 DE→EN test set. This result follows the setting of SEQDIFFUSEQ. “NFE” indicates the Number of Function Evaluations [Ye et al., 2023].

Methods	Pattern	BLEU	Steps	NFE ( $n \times$ Steps)
Transformer [Vaswani et al., 2017]	AR	34.74	-	-
CNAT [Bao et al., 2021]	NAR	29.81	-	-
SeqDiffuSeq ( $n = 1$ ) [Yuan et al., 2022]	Diffusion	29.83	2,000	2,000 ( $2,000 \times 1$ )
AR-DIFFUSION ( $n = 1$ )		30.19	20	20 ( $20 \times 1$ )
GENIE ( $n = 50$ ) [Lin et al., 2023]	Diffusion	30.08	20	1,000 ( $20 \times 50$ )
AR-DIFFUSION ( $n = 50$ )		<u>34.95</u>	20	1,000 ( $20 \times 50$ )
AR-DIFFUSION ( $n = 500$ )		<b>35.62</b>	20	10,000 ( $20 \times 500$ )

<sup>12</sup>Notably, although AR’s beam search has a small beam, the search space may be larger than 50 or even 500.

**Machine Translation** Table 4 presents the BLEU score implemented by SeqDiffuSeq setting. AR-DIFFUSION outperforms the non-auto-regressive CNAT in greedy search for a single sample, and achieves a substantial gain. Moreover, the BLEU score of AR-DIFFUSION surpasses GENIE by a large margin and shows a slightly better performance than the AR Transformer. Specially, AR-DIFFUSION achieves a more powerful result at  $n = 500$ .

In Table 5 we give the SacreBLEU score according to the setting of DINOISER. AR-DIFFUSION has notable improvements over non-auto-regressive CMLM. Besides, AR-DIFFUSION achieves excellent performance among text diffusion models for both EN→DE and DE→EN tasks. Specifically, AR-DIFFUSION is far superior to GENIE and comparable to the newly proposed DINOISER at  $n = 50$ . Nevertheless, the performance is stronger than DINOISER when  $n$  is 500<sup>13</sup>.

Table 5: SacreBLEU on the IWSLT14 test set. This result follows the setting of DINOISER.

Methods	IWSLT14	
	DE→EN	EN→DE
Transformer (AR, beam = 5) [Vaswani et al., 2017]	33.61	28.30
CMLM (NAR, $n = 5$ ) [Ghazvininejad et al., 2019]	29.41	24.34
DiffusionLM ( $n = 50$ ) [Li et al., 2022a]	29.11	22.91
DINOISER ( $n = 50$ ) [Ye et al., 2023]	31.61	<u>26.14</u>
GENIE ( $n = 50$ ) [Lin et al., 2023]	29.45	23.89
AR-DIFFUSION ( $n = 50$ )	<u>31.80</u>	26.01
AR-DIFFUSION ( $n = 500$ )	<b>32.35</b>	<b>26.51</b>

Table 6: Results on COMMONGEN dev set. Results of NAR and AR are from Lin et al. [2020]

Methods	Pattern	ROUGE-2/L		BLEU-3/4		METEOR	SPICE
bRNN-CopyNet [Gu et al., 2016]	AR	9.23	30.57	13.60	7.80	17.40	16.90
Trans-CopyNet [Lin et al., 2020]		11.08	32.57	17.20	10.60	18.80	18.00
MeanPooling-CopyNet [Lin et al., 2020]		11.36	34.63	14.80	8.90	19.20	20.20
LevT [Gu et al., 2019]	NAR	12.22	<u>35.42</u>	<u>23.10</u>	<u>15.00</u>	22.10	21.40
ConstLeven [Susanto et al., 2020]		<u>13.47</u>	35.19	21.30	12.30	<b>25.00</b>	<u>23.20</u>
GENIE ( $n = 50$ ) [Lin et al., 2023]	Diffusion	12.89	35.21	22.00	13.30	<u>24.30</u>	23.00
AR-DIFFUSION ( $n = 50$ )		<b>13.93</b>	<b>37.36</b>	<b>25.60</b>	<b>16.40</b>	<b>25.00</b>	<b>24.20</b>

**Common Sense Generation** As depicted in Table 6, AR-DIFFUSION achieves superior performance compared to the current AR, NAR, and Diffusion methods across all metrics on the COMMONGEN dataset.

#### 4.4 Analysis

**Inference Efficiency** Inference speed is a significant concern in diffusion models.

First, we use the number of function evaluations (NFE) as a measure of the total number of forward passes to compare inference efficiency [Ye et al., 2023] in machine translation. From Table 4, it is evident that even when the NFE is reduced to 1% of SeqDiffuSeq (equivalent to 100× faster), AR-DIFFUSION consistently outperforms SeqDiffuSeq. Moreover, increasing the number of candidate samples ( $n = 500$ ) leads to further performance improvements, albeit with increased time consumption.

Second, we conduct experiments with an **extremely limited number of inference steps** (2 and 3) and compare the performance with that of GENIE in XSUM. The results are presented in Table 7. When reducing the number of steps to 2, GENIE experiences a significant decline, with an average score of 4.20, while AR-DIFFUSION exhibits a comparatively smaller decrease of 1.34. Furthermore,

<sup>13</sup>DINOISER has shown in their Figure 4 that their method is not better with a larger  $n$ .

with 3 steps, although the performance deterioration of GENIE is somewhat reduced, the average score still shows a decline of 2.81. In contrast, AR-DIFFUSION maintains a high performance level, with an average score differing from the 20-step result by only 0.64. Notably, the results of AR-DIFFUSION at 3 steps are comparable to the results of GENIE at 2,000 steps. Therefore, compared to GENIE, the inference speed of AR-DIFFUSION can be accelerated by up to  $600\times$ .

Table 7: Experimental results of GENIE and AR-DIFFUSION with inference steps of **2** and **3** on XSUM test set. Take  $n = 10$  to apply the MBR decoding strategy. (·) indicates the **drop** score compared to the 20-step.

Methods	Steps	NFE	ROUGE-1	ROUGE-2	ROUGE-L	AVG Drop
GENIE	2,000	20,000	30.36	8.78	23.31	-
	20	200	28.33	7.46	21.15	-
	3	30	25.03 (-3.30)	5.32 (-2.14)	18.17 (-2.98)	2.81
	2	20	23.45 (-4.88)	3.95 (-3.51)	16.94 (-4.21)	4.20
AR-DIFFUSION	20	200	30.99	9.32	23.95	-
	3	30	30.23 (-0.76)	8.68 (-0.64)	23.43 (-0.52)	<b>0.64</b>
	2	20	29.28 (-1.71)	7.99 (-1.33)	22.98 (-0.97)	<b>1.34</b>

**Diversity of Samples** Diversity is a key advantage of diffusion models. To measure the diversity of generated samples, We adopt the SELF-BLEU [Zhu et al., 2018] metric, which a lower score indicates higher diversity. In Lin et al. [2023], various sampling methods were applied to the pre-trained autoregressive model BART, including Greedy Search, Beam Search Xiao et al. [2022], Diverse Beam Search (diversity strength = 0.8) Vijayakumar et al. [2016], Typical Sample ( $\tau = 1.2$ ) Meister et al. [2022], Top-k Sample ( $k = 50$ ) Fan et al. [2018] and Nucleus Sample ( $p = 0.92$ ) Holtzman et al. [2020].

Specifically, greedy search is to select the token with the highest probability at each step. Beam search is to select the largest token from among the beams with higher probability at each step. Diverse beam search is to divide the beams into multiple groups at each step and ensure the difference between groups by calculating the diversity score between groups. Typical sampling selects samples through a discrete random process. Top-k sampling is to randomly select one of the  $k$  candidate tokens with the highest probability at each step. Nucleus sampling is to randomly select one token at each step from the candidate tokens whose probability density is greater than  $p$ .

As shown in Table 8, AR-DIFFUSION achieves significantly higher diversity compared to AR model. Furthermore, the diversity can be comparable to GENIE with much better performance.

Table 8: Diversity of **10** generated samples on XSUM test set and average of **10** results. The results of AR and GENIE are quoted from Lin et al. [2023].

Methods	BART						GENIE	AR-DIFFUSION
	Greedy Search	Beam Search	Diverse Beam Search	Typical Sample	Top-k Sample	Nucleus Sample		
SELF-BLEU ↓	100.0	93.4	75.6	76.9	80.2	79.1	29.3	30.4

#### 4.5 Ablation Study

To demonstrate the effectiveness of our proposed methods, we perform ablation experiments on the XSUM dataset. Our results show that both our proposed token-level diffusion and skipping mechanism are essential for achieving the high performance of AR-DIFFUSION.

**Token-Level Diffusion** On the premise of maintaining the same inference method, we conducted an ablation experiment on the XSUM dataset by removing the token-level diffusion during training. The comparison results are shown in Figure 2(a). It can be observed that after removing the token-level diffusion, the AVG-ROUGE score has been greatly reduced, especially after 2 steps.

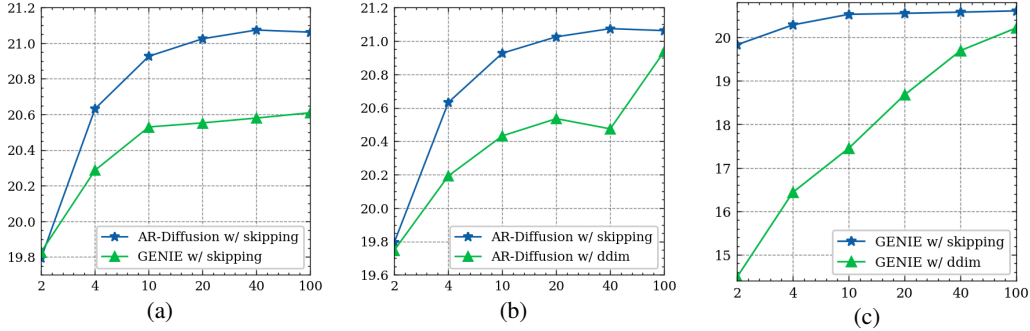


Figure 2: Ablation experiments on XSUM test set and taking  $n = 5$ . The horizontal axis is the number of inference steps and the vertical axis is  $\text{AVG-ROUGE} = (\text{ROUGE-1} + \text{ROUGE-2} + \text{ROUGE-L}) / 3$ .

**Skipping Mechanism** On the other hand, the performance of applying our proposed skipping and ddim to the same model is shown in Figure 2(b). The results demonstrate that skipping consistently outperforms ddim. Additionally, the skipping mechanism can be easily applied to other diffusion models. As shown in Figure 2(c), while ddim performs relatively well on GENIE at 100 inference steps, ddim suffers a significant drop in performance at 2 inference steps. In contrast, skipping maintains a consistently good performance across all inference steps.

#### 4.6 Impact of Minimum Bayes Risk and Anchor Point

**Minimum Bayes Risk** Experiments find that increasing the number of candidate samples can improve the quality of generation. In order to further explore the relationship between the two, we generate 1,000 samples on the IWSLT14 De→En test set and draw Figure 3. The curve illustrates that the gain of about 0.5 SacreBLEU points is provided in the first 200 samples, after which the gain is no longer significant with additional samples.

**Anchor Point** We also try several anchor points in different positions as shown in Table 9, and find that the best result when  $n_e$  is 2 times the target sentence length and  $t_e$  is the total time step of diffusion.

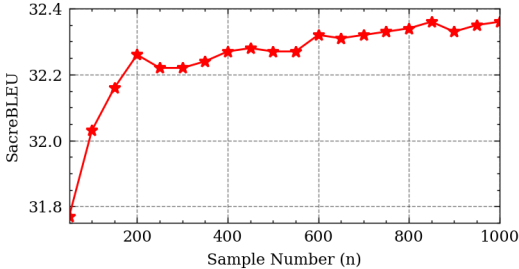


Figure 3: Correlation between the number of candidate samples for applying MBR and SacreBLEU on IWSLT14 DE→EN test set.

Table 9: Effect of anchor point at different positions on the IWSLT14 DE→EN test set. " $N$ " indicates the target sequence length.

$n_e$	$t_e$	SacreBLEU
$1.0 \times N$	2,000	31.23
$2.0 \times N$	2,000	<b>31.80</b>
$3.0 \times N$	2,000	31.58

#### 4.7 Case Study

Based on our motivation, the tokens on the left side should generate faster than those on the right side. We demonstrate the validity of AR-DIFFUSION by outputting intermediate states, as shown in Figure 4, where AR-DIFFUSION is denoised from a random standard Gaussian noise to a fluent sentence through 20 steps. As the timestep progresses, the logits of the tokens at the left of the sentence increase rapidly, quickly taking the form of the final output. The logits of the tokens in right positions of the sentence increase at a slower pace, allowing for the utilization of information from preceding tokens to transform into the final output.

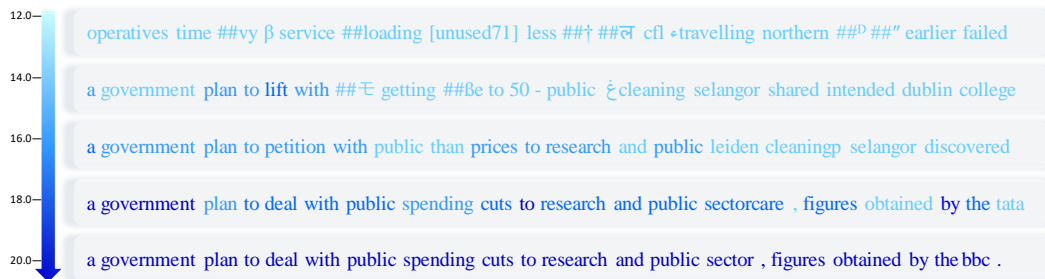


Figure 4: The intermediate state of AR-DIFFUSION gradually generating real text from a standard Gaussian noise through 20 steps. The brightness of the color represents the magnitude of the logits, with darker colors indicating larger logits.

## 5 Related Work

**AR and NAR Language Models** AR models have been the dominant approach for text generation [OpenAI, 2023, Touvron et al., 2023, Dong et al., 2023], but their token-by-token generation nature often leads to unsatisfactory inference speed. To address this issue, NAR models have been developed in recent years. The NAR method is initially proposed by Gu et al. [2017], its objective is generate the entire output sequence in parallel, rather than sequentially as in AR, thereby improving generation speed and efficiency. Subsequently, LevT [Gu et al., 2019] adopts insertion and deletion to address the lack of flexibility in NAR generation, CMLM [Ghazvininejad et al., 2019] utilizes a masked language model to improve the quality of NAR generation through a constant number of iterations, and CNAT [Bao et al., 2021] introduces latent variables to represent the category information of the target word to make full use of the latent representation. However, the NAR method generates tokens in one step, with no intermediate potential state. The diffusion model, which has been in full swing in the image field recently [Rombach et al., 2022, Saharia et al., 2022], provides a new solution for this purpose.

**Continuous Text Diffusion** The application of diffusion models to continuous text space is first introduced by Li et al. [2022a]. Through additional embedding and rounding processes, the direct integration of continuous noise into word embeddings was accomplished. After that, more people attempt to adopt continuous text diffusion model to solve the sequence-to-sequence task. DiffuSeq [Gong et al., 2022] divides the input into two parts, utilizing one part as a condition, and perturbs the other part with noise. CDCD [Dieleman et al., 2022] proposes score interpolation and time warping to allow diffusion model and Euclidean embedding to share the same loss function for training. ARDMs [Hoogeboom et al., 2022] samples from a predefined position permutations each time to determine the position where the token is generated. SeqDiffuSeq [Yuan et al., 2022], GENIE [Lin et al., 2023] and DINOISER [Ye et al., 2023] incorporate diffusion model into the encoder-decoder structure through cross-attention mechanisms. In this paper, our primary focus is on the application of continuous text diffusion through the encoder-decoder framework.

## 6 Conclusion

In this paper, we propose AR-DIFFUSION, a novel diffusion model for text generation. AR-DIFFUSION integrates the concepts of auto-regressive decoding and diffusion models through the implementation of the multi-level diffusion strategy. This strategy encompasses two levels of diffusion. The sentence-level diffusion is similar to the existing methods like Diffusion-LM. While in the token-level diffusion, we assign dynamic movement speeds for different tokens. Consequently, AR-DIFFUSION can utilize both the sequential order of the auto-regressive model and the parallel decoding of the diffusion model with a skipping mechanism. Experimental results on different text generation tasks show that AR-DIFFUSION outperforms the existing state-of-the-art and achieve 100x faster when maintaining comparable results to SeqDiffuSeq. Notably, AR-DIFFUSION can still perform well in the challenge situation with extremely few decoding steps where most of the baselines commonly fail.

## References

- OpenAI. GPT-4 technical report. *CoRR*, abs/2303.08774, 2023. doi: 10.48550/arXiv.2303.08774. URL <https://doi.org/10.48550/arXiv.2303.08774>.
- Hugo Touvron, Thibaut Lavril, Gautier Izacard, Xavier Martinet, Marie-Anne Lachaux, Timothée Lacroix, Baptiste Rozière, Naman Goyal, Eric Hambro, Faisal Azhar, Aurélien Rodriguez, Armand Joulin, Edouard Grave, and Guillaume Lample. Llama: Open and efficient foundation language models. *CoRR*, abs/2302.13971, 2023. doi: 10.48550/arXiv.2302.13971. URL <https://doi.org/10.48550/arXiv.2302.13971>.
- Rohan Taori, Ishaan Gulrajani, Tianyi Zhang, Yann Dubois, Xuechen Li, Carlos Guestrin, Percy Liang, and Tatsunori B. Hashimoto. Stanford alpaca: An instruction-following llama model. [https://github.com/tatsu-lab/stanford\\_alpaca](https://github.com/tatsu-lab/stanford_alpaca), 2023.
- Ashish Vaswani, Noam Shazeer, Niki Parmar, Jakob Uszkoreit, Llion Jones, Aidan N Gomez, Łukasz Kaiser, and Illia Polosukhin. Attention is all you need. In I. Guyon, U. Von Luxburg, S. Bengio, H. Wallach, R. Fergus, S. Vishwanathan, and R. Garnett, editors, *Advances in Neural Information Processing Systems*, volume 30. Curran Associates, Inc., 2017. URL [https://proceedings.neurips.cc/paper\\_files/paper/2017/file/3f5ee243547dee91fbd053c1c4a845aa-Paper.pdf](https://proceedings.neurips.cc/paper_files/paper/2017/file/3f5ee243547dee91fbd053c1c4a845aa-Paper.pdf).
- Tom Brown, Benjamin Mann, Nick Ryder, Melanie Subbiah, Jared D Kaplan, Prafulla Dhariwal, Arvind Neelakantan, Pranav Shyam, Girish Sastry, Amanda Askell, et al. Language models are few-shot learners. *Advances in neural information processing systems*, 33:1877–1901, 2020.
- Jonathan Ho, Ajay Jain, and Pieter Abbeel. Denoising diffusion probabilistic models. In Hugo Larochelle, Marc’Aurelio Ranzato, Raia Hadsell, Maria-Florina Balcan, and Hsuan-Tien Lin, editors, *Advances in Neural Information Processing Systems 33: Annual Conference on Neural Information Processing Systems 2020, NeurIPS 2020, December 6-12, 2020, virtual*, 2020. URL <https://proceedings.neurips.cc/paper/2020/hash/4c5bcfec8584af0d967f1ab10179ca4b-Abstract.html>.
- Xiang Lisa Li, John Thickstun, Ishaan Gulrajani, Percy Liang, and Tatsunori Hashimoto. Diffusion-LM improves controllable text generation. In Alice H. Oh, Alekh Agarwal, Danielle Belgrave, and Kyunghyun Cho, editors, *Advances in Neural Information Processing Systems*, 2022a. URL <https://openreview.net/forum?id=3s9IrEsjLyk>.
- Shansan Gong, Mukai Li, Jiangtao Feng, Zhiyong Wu, and Lingpeng Kong. Diffuseq: Sequence to sequence text generation with diffusion models. *CoRR*, abs/2210.08933, 2022. doi: 10.48550/arXiv.2210.08933. URL <https://doi.org/10.48550/arXiv.2210.08933>.
- Sander Dieleman, Laurent Sartran, Arman Roshannai, Nikolay Savinov, Yaroslav Ganin, Pierre H Richemond, Arnaud Doucet, Robin Strudel, Chris Dyer, Conor Durkan, et al. Continuous diffusion for categorical data. *arXiv preprint arXiv:2211.15089*, 2022.
- Hongyi Yuan, Zheng Yuan, Chuanqi Tan, Fei Huang, and Songfang Huang. Seqdiffuseq: Text diffusion with encoder-decoder transformers, 2022.
- Jiasheng Ye, Zaixiang Zheng, Yu Bao, Lihua Qian, and Mingxuan Wang. Dinoiser: Diffused conditional sequence learning by manipulating noises, 2023.
- Mike Lewis, Yinhan Liu, Naman Goyal, Marjan Ghazvininejad, Abdelrahman Mohamed, Omer Levy, Veselin Stoyanov, and Luke Zettlemoyer. BART: denoising sequence-to-sequence pre-training for natural language generation, translation, and comprehension. In Dan Jurafsky, Joyce Chai, Natalie Schluter, and Joel R. Tetreault, editors, *Proceedings of the 58th Annual Meeting of the Association for Computational Linguistics, ACL 2020, Online, July 5-10, 2020*, pages 7871–7880. Association for Computational Linguistics, 2020. doi: 10.18653/v1/2020.acl-main.703. URL <https://doi.org/10.18653/v1/2020.acl-main.703>.
- Weizhen Qi, Yu Yan, Yeyun Gong, Dayiheng Liu, Nan Duan, Jiusheng Chen, Ruofei Zhang, and Ming Zhou. ProphetNet: Predicting future n-gram for sequence-to-SequencePre-training. In *Findings of the Association for Computational Linguistics: EMNLP 2020*, pages 2401–2410,

- Online, November 2020. Association for Computational Linguistics. doi: 10.18653/v1/2020.findings-emnlp.217. URL <https://aclanthology.org/2020.findings-emnlp.217>.
- Weizhen Qi, Yeyun Gong, Jian Jiao, Yu Yan, Weizhu Chen, Dayiheng Liu, Kewen Tang, Houqiang Li, Jiusheng Chen, Ruofei Zhang, et al. Bang: Bridging autoregressive and non-autoregressive generation with large scale pretraining. In *International Conference on Machine Learning*, pages 8630–8639. PMLR, 2021.
- Junyi Li, Tianyi Tang, Wayne Xin Zhao, Jian-Yun Nie, and Ji-Rong Wen. ELMER: A non-autoregressive pre-trained language model for efficient and effective text generation. In Yoav Goldberg, Zornitsa Kozareva, and Yue Zhang, editors, *Proceedings of the 2022 Conference on Empirical Methods in Natural Language Processing, EMNLP 2022, Abu Dhabi, United Arab Emirates, December 7-11, 2022*, pages 1044–1058. Association for Computational Linguistics, 2022b. URL <https://aclanthology.org/2022.emnlp-main.68>.
- Yafu Li, Leyang Cui, Yongjing Yin, and Yue Zhang. Multi-granularity optimization for non-autoregressive translation. In Yoav Goldberg, Zornitsa Kozareva, and Yue Zhang, editors, *Proceedings of the 2022 Conference on Empirical Methods in Natural Language Processing, EMNLP 2022, Abu Dhabi, United Arab Emirates, December 7-11, 2022*, pages 5073–5084. Association for Computational Linguistics, 2022c. URL <https://aclanthology.org/2022.emnlp-main.339>.
- Yu Bao, Shujian Huang, Tong Xiao, Dongqi Wang, Xinyu Dai, and Jiajun Chen. Non-autoregressive translation by learning target categorical codes. In *Proceedings of the 2021 Conference of the North American Chapter of the Association for Computational Linguistics: Human Language Technologies*, pages 5749–5759, Online, June 2021. Association for Computational Linguistics. doi: 10.18653/v1/2021.naacl-main.458. URL <https://aclanthology.org/2021.naacl-main.458>.
- Zhenghao Lin, Yeyun Gong, Yelong Shen, Tong Wu, Zhihao Fan, Chen Lin, Nan Duan, and Weizhu Chen. Text generation with diffusion language models: A pre-training approach with continuous paragraph denoise, 2023.
- Jiatao Gu, James Bradbury, Caiming Xiong, Victor OK Li, and Richard Socher. Non-autoregressive neural machine translation. *arXiv preprint arXiv:1711.02281*, 2017.
- Shashi Narayan, Shay B. Cohen, and Mirella Lapata. Don’t give me the details, just the summary! topic-aware convolutional neural networks for extreme summarization. In *Proceedings of the 2018 Conference on Empirical Methods in Natural Language Processing*, pages 1797–1807, Brussels, Belgium, October-November 2018. Association for Computational Linguistics. doi: 10.18653/v1/D18-1206. URL <https://aclanthology.org/D18-1206>.
- Karl Moritz Hermann, Tomas Kocisky, Edward Grefenstette, Lasse Espeholt, Will Kay, Mustafa Suleyman, and Phil Blunsom. Teaching machines to read and comprehend. In C. Cortes, N. Lawrence, D. Lee, M. Sugiyama, and R. Garnett, editors, *Advances in Neural Information Processing Systems*, volume 28. Curran Associates, Inc., 2015. URL [https://proceedings.neurips.cc/paper\\_files/paper/2015/file/afdec7005cc9f14302cd0474fd0f3c96-Paper.pdf](https://proceedings.neurips.cc/paper_files/paper/2015/file/afdec7005cc9f14302cd0474fd0f3c96-Paper.pdf).
- Taku Kudo and John Richardson. SentencePiece: A simple and language independent subword tokenizer and detokenizer for neural text processing. In *Proceedings of the 2018 Conference on Empirical Methods in Natural Language Processing: System Demonstrations*, pages 66–71, Brussels, Belgium, November 2018. Association for Computational Linguistics. doi: 10.18653/v1/D18-2012. URL <https://aclanthology.org/D18-2012>.
- Jason Lee, Elman Mansimov, and Kyunghyun Cho. Deterministic non-autoregressive neural sequence modeling by iterative refinement. *arXiv preprint arXiv:1802.06901*, 2018.
- Marjan Ghazvininejad, Omer Levy, Yinhan Liu, and Luke Zettlemoyer. Mask-predict: Parallel decoding of conditional masked language models. In *Proceedings of the 2019 Conference on Empirical Methods in Natural Language Processing and the 9th International Joint Conference on Natural Language Processing (EMNLP-IJCNLP)*, pages 6112–6121, Hong Kong, China, November 2019. Association for Computational Linguistics. doi: 10.18653/v1/D19-1633. URL <https://aclanthology.org/D19-1633>.

- Jiatao Gu, Changhan Wang, and Junbo Zhao. Levenshtein transformer. In *Advances in Neural Information Processing Systems*, pages 11181–11191, 2019.
- Mitchell Stern, William Chan, Jamie Kiros, and Jakob Uszkoreit. Insertion transformer: Flexible sequence generation via insertion operations. *arXiv preprint arXiv:1902.03249*, 2019.
- Jiatao Gu, Zhengdong Lu, Hang Li, and Victor O. K. Li. Incorporating copying mechanism in sequence-to-sequence learning. In *ACL (1)*. The Association for Computer Linguistics, 2016.
- Klaus Greff, Rupesh Kumar Srivastava, Jan Koutník, Bas R. Steunebrink, and Jürgen Schmidhuber. LSTM: A search space odyssey. *IEEE Trans. Neural Networks Learn. Syst.*, 28(10):2222–2232, 2017.
- Bill Yuchen Lin, Wangchunshu Zhou, Ming Shen, Pei Zhou, Chandra Bhagavatula, Yejin Choi, and Xiang Ren. CommonGen: A constrained text generation challenge for generative commonsense reasoning. In *Findings of the Association for Computational Linguistics: EMNLP 2020*, pages 1823–1840, Online, November 2020. Association for Computational Linguistics. doi: 10.18653/v1/2020.findings-emnlp.165. URL <https://aclanthology.org/2020.findings-emnlp.165>.
- Shankar Kumar and William Byrne. Minimum bayes-risk decoding for statistical machine translation. Technical report, JOHNS HOPKINS UNIV BALTIMORE MD CENTER FOR LANGUAGE AND SPEECH PROCESSING (CLSP), 2004.
- Dayiheng Liu, Yu Yan, Yeyun Gong, Weizhen Qi, Hang Zhang, Jian Jiao, Weizhu Chen, Jie Fu, Linjun Shou, Ming Gong, et al. Glge: A new general language generation evaluation benchmark. In *Findings of the Association for Computational Linguistics: ACL-IJCNLP 2021*, pages 408–420, 2021.
- Raymond Hendy Susanto, Shamil Chollampatt, and Liling Tan. Lexically constrained neural machine translation with levenshtein transformer. In *ACL*, pages 3536–3543. Association for Computational Linguistics, 2020.
- Yaoming Zhu, Sidi Lu, Lei Zheng, Jiaxian Guo, Weinan Zhang, Jun Wang, and Yong Yu. Tegygen: A benchmarking platform for text generation models. In *The 41st international ACM SIGIR conference on research & development in information retrieval*, pages 1097–1100, 2018.
- Yisheng Xiao, Lijun Wu, Junliang Guo, Juntao Li, Min Zhang, Tao Qin, and Tie-Yan Liu. A survey on non-autoregressive generation for neural machine translation and beyond. *CoRR*, abs/2204.09269, 2022.
- Ashwin K. Vijayakumar, Michael Cogswell, Ramprasaath R. Selvaraju, Qing Sun, Stefan Lee, David J. Crandall, and Dhruv Batra. Diverse beam search: Decoding diverse solutions from neural sequence models. *CoRR*, abs/1610.02424, 2016.
- Clara Meister, Tiago Pimentel, Gian Wiher, and Ryan Cotterell. Typical decoding for natural language generation. *CoRR*, abs/2202.00666, 2022.
- Angela Fan, Mike Lewis, and Yann N. Dauphin. Hierarchical neural story generation. In *ACL (1)*, pages 889–898. Association for Computational Linguistics, 2018.
- Ari Holtzman, Jan Buys, Li Du, Maxwell Forbes, and Yejin Choi. The curious case of neural text degeneration. In *ICLR*. OpenReview.net, 2020.
- Chenhe Dong, Yinghui Li, Haifan Gong, Miaoxin Chen, Junxin Li, Ying Shen, and Min Yang. A survey of natural language generation. *ACM Comput. Surv.*, 55(8):173:1–173:38, 2023. doi: 10.1145/3554727. URL <https://doi.org/10.1145/3554727>.
- Robin Rombach, Andreas Blattmann, Dominik Lorenz, Patrick Esser, and Björn Ommer. High-resolution image synthesis with latent diffusion models. In *Proceedings of the IEEE/CVF Conference on Computer Vision and Pattern Recognition (CVPR)*, pages 10684–10695, June 2022.

- Chitwan Saharia, William Chan, Saurabh Saxena, Lala Li, Jay Whang, Emily L Denton, Kamyar Ghasemipour, Raphael Gontijo Lopes, Burcu Karagol Ayan, Tim Salimans, Jonathan Ho, David J Fleet, and Mohammad Norouzi. Photorealistic text-to-image diffusion models with deep language understanding. In S. Koyejo, S. Mohamed, A. Agarwal, D. Belgrave, K. Cho, and A. Oh, editors, *Advances in Neural Information Processing Systems*, volume 35, pages 36479–36494. Curran Associates, Inc., 2022. URL [https://proceedings.neurips.cc/paper\\_files/paper/2022/file/ec795aeadae0b7d230fa35cbaf04c041-Paper-Conference.pdf](https://proceedings.neurips.cc/paper_files/paper/2022/file/ec795aeadae0b7d230fa35cbaf04c041-Paper-Conference.pdf).
- Emiel Hoogeboom, Alexey A. Gritsenko, Jasmijn Bastings, Ben Poole, Rianne van den Berg, and Tim Salimans. Autoregressive diffusion models. In *International Conference on Learning Representations*, 2022. URL <https://openreview.net/forum?id=Lm8T39vLDTE>.
- Calvin Luo. Understanding diffusion models: A unified perspective. *arXiv preprint arXiv:2208.11970*, 2022.

## A Proof of Inference with Skipping

Through maximizing the evidence lower bound (ELBO) of  $p(\mathbf{z}_0)$ , the training object is equivalent to minimize the divergence between  $q(\mathbf{z}_t|\mathbf{z}_{t-1}, \mathbf{z}_0)$  and  $p_\theta(\mathbf{z}_{t-1}|\mathbf{z}_t)$  following [Luo, 2022].

By converting the joint probability distribution into a conditional probability distribution, we obtain the following formula for  $q(\mathbf{z}_{t_{i+1}}|\mathbf{z}_{t_i}, \mathbf{z}_0)$ .

$$\begin{aligned}
q(\mathbf{z}_{t_{i+1}}|\mathbf{z}_{t_i}, \mathbf{z}_0) &= q(\mathbf{z}_{t_{i+1}}|\mathbf{z}_{t_i-1}, \mathbf{z}_{t_i}, \mathbf{z}_0) q(\mathbf{z}_{t_{i+1}-1}|\mathbf{z}_{t_i}, \mathbf{z}_0) \\
&= q(\mathbf{z}_{t_{i+1}}|\mathbf{z}_{t_i-1}, \mathbf{z}_0) q(\mathbf{z}_{t_{i+1}-1}|\mathbf{z}_{t_i}, \mathbf{z}_0) \\
&= q(\mathbf{z}_{t_{i+1}}|\mathbf{z}_{t_i-2}, \mathbf{z}_0) q(\mathbf{z}_{t_{i+1}-2}|\mathbf{z}_{t_i-1}, \mathbf{z}_0) q(\mathbf{z}_{t_{i+1}-1}|\mathbf{z}_{t_i}, \mathbf{z}_0) \\
&= \prod_{k=1}^{t_i-t_{i+1}} q(\mathbf{z}_{t_i-k}|\mathbf{z}_{t_i-k+1}, \mathbf{z}_0)
\end{aligned} \tag{13}$$

Similarly, we reach the same conclusion regarding  $p_\theta(\mathbf{z}_{t_{i+1}}|\mathbf{z}_{t_i})$ .

Based on equation (13), which consists of  $q(\mathbf{z}_t|\mathbf{z}_{t-1}, \mathbf{z}_0)$ , and the interchangeability between  $q(\mathbf{z}_i|\mathbf{z}_{i-1}, \mathbf{z}_0)$  and  $p_\theta(\mathbf{z}_{i-1}|\mathbf{z}_i)$ , we can decompose  $q(\mathbf{z}_{t_{i+1}}|\mathbf{z}_{t_i}, \mathbf{z}_0)$  by incorporating  $\mathbf{z}_{t_i}$  and  $\mathbf{z}_0$ , and utilize our estimated  $\mathbf{z}_0$  to determine the expression of  $p_\theta(\mathbf{z}_{t_{i+1}}|\mathbf{z}_{t_i})$ .

$$q(\mathbf{z}_{t_{i+1}}|\mathbf{z}_{t_i}, \mathbf{z}_0) = \prod_{n=1}^N q(z_{f(n,t_{i+1})}^n | z_{f(n,t_i)}^n, z_0^n) \tag{14}$$

Next, we obtain the explicit expression  $q(z_{f(n,t_{i+1})}^n | z_{f(n,t_i)}^n, z_0^n)$  through linear interpolation between  $z_{f(n,t_i)}^n$  and  $z_0^n$ .

$$\begin{aligned}
q(z_{f(n,t_{i+1})}^n | z_{f(n,t_i)}^n, z_0^n) &= \frac{q(z_{f(n,t_i)}^n | z_{f(n,t_{i+1})}^n, z_0^n) q(z_{f(n,t_{i+1})}^n | z_0^n)}{q(z_{f(n,t_i)}^n | z_0^n)} \\
&= \frac{\mathcal{N}\left(z_{f(n,t_i)}^n; \sqrt{\frac{\bar{\alpha}_{f(n,t_i)}}{\bar{\alpha}_{f(n,t_{i+1})}}} z_{f(n,t_{i+1})}^n, (1 - \frac{\bar{\alpha}_{f(n,t_i)}}{\bar{\alpha}_{f(n,t_{i+1})}}) I\right) \mathcal{N}\left(z_{f(n,t_{i+1})}^n; \sqrt{\bar{\alpha}_{f(n,t_{i+1})}} z_0^n, (1 - \bar{\alpha}_{f(n,t_{i+1})}) I\right)}{\mathcal{N}\left(z_{f(n,t_i)}^n; \sqrt{\bar{\alpha}_{f(n,t_i)}} z_0^n, (1 - \bar{\alpha}_{f(n,t_i)}) I\right)} \\
&\propto \exp \left\{ -\frac{(z_{f(n,t_i)}^n - \sqrt{\frac{\bar{\alpha}_{f(n,t_i)}}{\bar{\alpha}_{f(n,t_{i+1})}}} z_{f(n,t_{i+1})}^n)^2}{2(1 - \frac{\bar{\alpha}_{f(n,t_i)}}{\bar{\alpha}_{f(n,t_{i+1})}})} - \frac{(z_{f(n,t_{i+1})}^n - \sqrt{\bar{\alpha}_{f(n,t_{i+1})}} z_0^n)^2}{1 - \bar{\alpha}_{f(n,t_{i+1})}} \right. \\
&\quad \left. + \frac{(z_{f(n,t_i)}^n - \sqrt{\bar{\alpha}_{f(n,t_i)}} z_0^n)^2}{1 - \bar{\alpha}_{f(n,t_i)}} \right\} \\
&= \exp \left\{ -\frac{1 - \bar{\alpha}_{f(n,t_i)}}{2(1 - \frac{\bar{\alpha}_{f(n,t_i)}}{\bar{\alpha}_{f(n,t_{i+1})}})(1 - \bar{\alpha}_{f(n,t_{i+1})})} \left[ z_{f(n,t_{i+1})}^n \right]^2 - 2 \left( \frac{\sqrt{\frac{\bar{\alpha}_{f(n,t_i)}}{\bar{\alpha}_{f(n,t_{i+1})}}}(1 - \bar{\alpha}_{f(n,t_{i+1})})}{1 - \bar{\alpha}_{f(n,t_i)}} z_{f(n,t_i)}^n \right. \right. \\
&\quad \left. \left. + \frac{\sqrt{\bar{\alpha}_{f(n,t_{i+1})}}(1 - \frac{\bar{\alpha}_{f(n,t_i)}}{\bar{\alpha}_{f(n,t_{i+1})}})}{1 - \bar{\alpha}_{f(n,t_i)}} z_0^n \right) z_{f(n,t_{i+1})}^n \right\} \\
&\propto \mathcal{N}\left(z_{f(n,t_{i+1})}^n; \frac{\sqrt{\frac{\bar{\alpha}_{f(n,t_i)}}{\bar{\alpha}_{f(n,t_{i+1})}}}(1 - \bar{\alpha}_{f(n,t_{i+1})})}{1 - \bar{\alpha}_{f(n,t_i)}} z_{f(n,t_i)}^n + \frac{\sqrt{\bar{\alpha}_{f(n,t_{i+1})}}(1 - \frac{\bar{\alpha}_{f(n,t_i)}}{\bar{\alpha}_{f(n,t_{i+1})}})}{1 - \bar{\alpha}_{f(n,t_i)}} z_0^n, \right. \\
&\quad \left. \frac{(1 - \frac{\bar{\alpha}_{f(n,t_i)}}{\bar{\alpha}_{f(n,t_{i+1})}})(1 - \bar{\alpha}_{f(n,t_{i+1})})}{1 - \bar{\alpha}_{f(n,t_i)}} I\right) \\
&= \mathcal{N}(z_{f(n,t_{i+1})}^n; \lambda z_{f(n,t_i)}^n + \mu z_0^n, \sigma I)
\end{aligned} \tag{15}$$

where we have the following notations for simplification.

$$\lambda = \frac{\sqrt{\frac{\bar{\alpha}_{f(n,t_i)}}{\bar{\alpha}_{f(n,t_{i+1})}}}(1 - \bar{\alpha}_{f(n,t_{i+1})})}{1 - \bar{\alpha}_{f(n,t_i)}}, \quad \mu = \frac{\sqrt{\bar{\alpha}_{f(n,t_{i+1})}}(1 - \frac{\bar{\alpha}_{f(n,t_i)}}{\bar{\alpha}_{f(n,t_{i+1})}})}{1 - \bar{\alpha}_{f(n,t_i)}}, \quad \sigma = \frac{(1 - \alpha_{f(n,t_i)})(1 - \bar{\alpha}_{f(n,t_{i+1})})}{1 - \bar{\alpha}_{f(n,t_i)}}$$

Building upon equation (15), we substitute  $\mathbf{z}_0^n$  with  $\mathbf{g}_\theta(\mathbf{z}_{f(n,t)}^n, f(n, t); \mathbf{x})$ , yielding the final formula for  $p_\theta(\mathbf{z}_{f(n,t_{i+1})}^n | \mathbf{z}_{f(n,t_i)}^n; \mathbf{x})$  as the following equation.

$$p_\theta(\mathbf{z}_{f(n,t_{i+1})}^n | \mathbf{z}_{f(n,t_i)}^n; \mathbf{x}) \sim \mathcal{N}(\mathbf{z}_{f(n,t_{i+1})}^n; \lambda \mathbf{z}_{f(n,t_i)}^n + \mu \mathbf{g}_\theta(\mathbf{z}_{f(n,t)}^n, f(n, t); \mathbf{x}), \sigma \mathbf{I}) \quad (16)$$